The Dendritic Branch Is the Preferred Integrative Unit for Protein Synthesis-Dependent LTP

Arvind Govindarajan,[1,2] Inbal Israely,[1,2,3] Shu-Ying Huang,[1] and Susumu Tonegawa[1,*]
[1]The Picower Institute for Learning and Memory, RIKEN-MIT Center for Neural Circuit Genetics, Department of Biology
and Department of Brain and Cognitive Sciences, Massachusetts Institute of Technology, Cambridge, MA 02139, USA
[2]These authors contributed equally to this work
[3]Present address: Champalimaud Neuroscience Program, Instituto Gulbenkian de Ciencia, Rua da Quinta Grande, 6, 2780-156 Oeiras, Portugal
*Correspondence: tonegawa@mit.edu
DOI 10.1016/j.neuron.2010.12.008

SUMMARY

The late-phase of long-term potentiation (L-LTP), the cellular correlate of long-term memory, induced at some synapses facilitates L-LTP expression at other synapses receiving stimulation too weak to induce L-LTP by itself. Using glutamate uncaging and two-photon imaging, we demonstrate that the efficacy of this facilitation decreases with increasing time between stimulations, increasing distance between stimulated spines and with the spines being on different dendritic branches. Paradoxically, stimulated spines compete for L-LTP expression if stimulated too closely together in time. Furthermore, the facilitation is temporally bidirectional but asymmetric. Additionally, L-LTP formation is itself biased toward occurring on spines within a branch. These data support the Clustered Plasticity Hypothesis, which states that such spatial and temporal limits lead to stable engram formation, preferentially at synapses clustered within dendritic branches rather than dispersed throughout the dendritic arbor. Thus, dendritic branches rather than individual synapses are the primary functional units for long-term memory storage.

INTRODUCTION

Changes in synaptic weights and neuronal excitability are considered to be the neural substrates for the storage of memory engrams (Johnston and Narayanan, 2008; Malenka and Bear, 2004). Studies using extracellular field recordings and field stimulations at the Schaffer collateral-CA1 synapse have led to the synaptic tagging and capture (STC) model. This model states that synapses at which any form of long-term potentiation (LTP) (i.e., the longer lasting, protein synthesis-dependent late-phase of long-term potentiation [L-LTP], and the shorter lasting, protein synthesis-independent E-LTP) is induced become tagged in a protein synthesis-independent manner. The induction of L-LTP leads to protein synthesis, and all tagged synapses can use the resulting plasticity-related protein products (PrPs) to

express L-LTP (Frey and Morris, 1997, 1998). This facilitation is time limited and occurs regardless of whether the E-LTP-inducing stimulation precedes the L-LTP-inducing stimulation or vice versa (Frey and Morris, 1997). However, much remains unknown about the temporal and spatial restriction of the facilitation and various parameters that affect its strength. Importantly, several models postulate that STC works via somatically synthesized PrPs available to synapses throughout the neuron (Barrett et al., 2009; Clopath et al., 2008; Frey, 2001; Frey and Morris, 1997; Okada et al., 2009). This, in turn, would lead to a memory engram being formed, at the single-cell level, at synapses dispersed throughout the dendritic arbor. However, an alternative model combining STC with the phenomenon of local activity-induced protein synthesis (Martin and Kosik, 2002; Steward and Schuman, 2001), namely the Clustered Plasticity Hypothesis (CPH) (Govindarajan et al., 2006), predicts that STC is biased toward occurring between spines that are close together. This would result in memory engrams being preferentially formed at synapses clustered within dendritic compartments, such as a branch (Govindarajan et al., 2006). Competition among synapses for limiting PrPs would further restrict the engram to such a dendritic compartment because spines close to the site of translation would use up limiting PrPs and reduce their concentration at more distant spines (Govindarajan et al., 2006). The advantages of the CPH include increased efficiency of long-term memory formation and retrieval, as well as a greater capacity for memory storage for an individual neuron (Govindarajan et al., 2006).

A study of the link between the level of E-LTP at a given spine and the strength of its synaptic tag, the spatial limits over which STC can occur, and the temporal dynamics of the STC at individual stimulated competing spines require a method that permits stimulations and response monitoring of single spines. However, the field stimulation and field recording methods that have been used in the past to study STC measure the average response of a population of unidentified stimulated synapses. Thus, we developed a method using two-photon glutamate uncaging at single spines on proximal apical dendritic branches of CA1 pyramidal neurons to examine the relationship between spines that participate in STC. The expression of L-LTP was assayed by examining spine volume using two-photon imaging of the fluorescent protein Dendra (Gurskaya et al., 2006), along with perforated patch-clamp electrophysiology in some experiments to measure the change in the postsynaptic response to

the uncaging of glutamate. We found that STC is temporally asymmetric, is spatially localized, and is biased toward occurring between stimulated spines that reside on the same dendritic branch. In addition, while strongly stimulated spines facilitate induction of L-LTP at neighboring weakly stimulated spines, the stimulated spines then compete for expression of L-LTP. Lastly, we demonstrated that there is a bias toward L-LTP being induced at a single dendritic branch, as opposed to across branches. Thus, to our knowledge, we provide the first experimental evidence in support of the CPH suggesting that, at the single-cell level, the dendritic branch is the primary unit for long-term memory engram storage.

RESULTS

L-LTP and STC Can Be Induced and Monitored at the Single-Spine Level

L-LTP in acute slices can be induced by the use of multiple-spaced electrical tetani (Frey et al., 1988; Huang and Kandel, 1994). It is well established that this L-LTP is dependent on dopamine receptor 1 (D1R) class activation (Frey et al., 1990, 1991; O'Carroll and Morris, 2004; Otmakhova and Lisman, 1996; Sajikumar and Frey, 2004; Sajikumar et al., 2008; Smith et al., 2005; Swanson-Park et al., 1999) and the PKA pathway (Abel et al., 1997; Huang and Kandel, 1994). Antagonists of either pathway present during the delivery of the tetani result in the expression of only E-LTP. Presumably the electrical stimulation is activating VTA terminals that are present in the slice (O'Carroll and Morris, 2004). Thus, multiple-spaced tetani likely lead to two parallel phenomena—a protein synthesis-independent E-LTP and a protein synthesis-dependent LTP, which we call L-LTP, that are separable. Conversely, the use of D1R (O'Carroll and Morris, 2004; Otmakhova and Lisman, 1996; Smith et al., 2005), PKA (Frey et al., 1993), and β-adrenergic agonists (Gelinas and Nguyen, 2005) along with weak electrical stimulation, or the use of BDNF (Kang and Schuman, 1995, 1996), results in the induction and expression of a purely protein synthesis-dependent LTP without E-LTP being induced simultaneously.

Because we were interested in studying L-LTP and STC at single visually identified spines, we chose glutamate uncaging targeted to a single spine in lieu of weak electrical stimulation of Schaffer collateral axons. Specifically, we combined a tetanus of glutamate uncaging (thirty 4 ms pulses at 0.5 Hz) in the absence of Mg^{+2} (Harvey and Svoboda, 2007; Harvey et al., 2008), concomitant with bath application of the PKA pathway agonist forskolin (which we will refer to as GLU+FSK stimulation) in order to induce L-LTP. This method provided a single-stimulus L-LTP induction protocol that differed from the E-LTP induction protocol, namely a tetanus in the absence of forskolin (which we will refer to as GLU stimulation), in only one component (i.e., forskolin). This allowed us to explore interactions between L-LTP and E-LTP without changing multiple parameters. Unlike the multiple electric tetanic stimulation protocol, which induces both E-LTP and L-LTP, the GLU+FSK stimulation protocol was expected to induce only L-LTP (Frey et al., 1993). Thus, we were able to study the effects of L-LTP induction at given spines on other spines without the confound of E-LTP also being induced simultaneously.

The GLU+FSK stimulation induced a significant change in the volume of the stimulated spine, without affecting neighboring spines (Figures 1A and 1B; see Figures S1A, S1B, and S1E available online, somatic potential change in response to uncaging pulse shown in Figure S1G). This change in volume accompanied a change in excitatory postsynaptic current (uEPSC) amplitude, measured using the perforated-patch technique (Figure 1B; Figure S1B), indicating that our protocol induced LTP, and not only a spine volume change. This was supported by our finding that the change in spine volume and that of uEPSC amplitude were well correlated (Figures S1C and S1D). As expected the presence of either protein synthesis (translation) inhibitor anisomycin or cycloheximide completely abolished the spine volume change (Figures 1C and 1D), mirroring field recording stimulation data (Frey et al., 1988). These data confirmed that the GLU+FSK stimulation protocol induced L-LTP, and not protein synthesis-independent E-LTP (Frey et al., 1988; Kelleher et al., 2004). In agreement with previous studies (Harvey and Svoboda, 2007; Harvey et al., 2008; Honkura et al., 2008; Lee et al., 2009; Matsuzaki et al., 2004; Yasuda et al., 2006), we found that GLU stimulation (somatic potential change in response to uncaging pulse shown in S1G) resulted in E-LTP induction, namely a robust protein synthesis-independent increase in spine volume (Figure 1E). However, the induced E-LTP returned to baseline within 2.5 hr, whereas the expression of L-LTP, induced by GLU+FSK stimulation, was maintained for at least 4 hr (Figure 1E; Figure S1E, and S1F).

As mentioned above, bath application of the D1R agonist SKF38393 along with weak electrical stimulation has been shown to induce a robust L-LTP via activation of the PKA pathway (O'Carroll and Morris, 2004; Otmakhova and Lisman, 1996; Smith et al., 2005). In line with these previous reports, when we bath applied SKF38393 instead of forskolin along with tetanic glutamate uncaging at a specific spine (GLU+SKF stimulation), the stimulated spine enlarged to a similar extent as the enlargement seen with L-LTP induced by GLU+FSK stimulation (Figure 1F).

In the search for evidence supporting the CPH, we had to first establish that STC can occur at individual spines and to determine its parameters. Thus, we applied GLU+FSK stimulation to one spine (L1), followed by GLU+FSK stimulation to a second spine (L2) 40 min later in the presence of anisomycin (Figures 2A–2C) or cycloheximide (Figure S2B). In both cases, L2 showed the same level of growth as L1 (Figures 2B and 2C; Figure S2B). This growth of L2 depended on protein synthesis induced in response to L1 stimulation because no growth was seen at either L1 or L2 if protein synthesis was blocked throughout the experiment using either anisomycin (Figure 2D) or cycloheximide (Figure S2C). Unstimulated spines showed no change in spine volume (data not shown). Neither the single-spine induction of L-LTP nor the single-spine STC phenomena were artifacts of the slice culture system, as they could also be induced in acute cut hippocampal slices (Figures S2D and S2E). These data demonstrate that STC occurs under single-spine stimulation conditions.

We wanted to confirm that the observed spine volume changes in response to L1 and L2 stimulations were correlated with electrophysiologically measured changes. Due to significant technical challenges of maintaining a cell in a perforated-patched state for
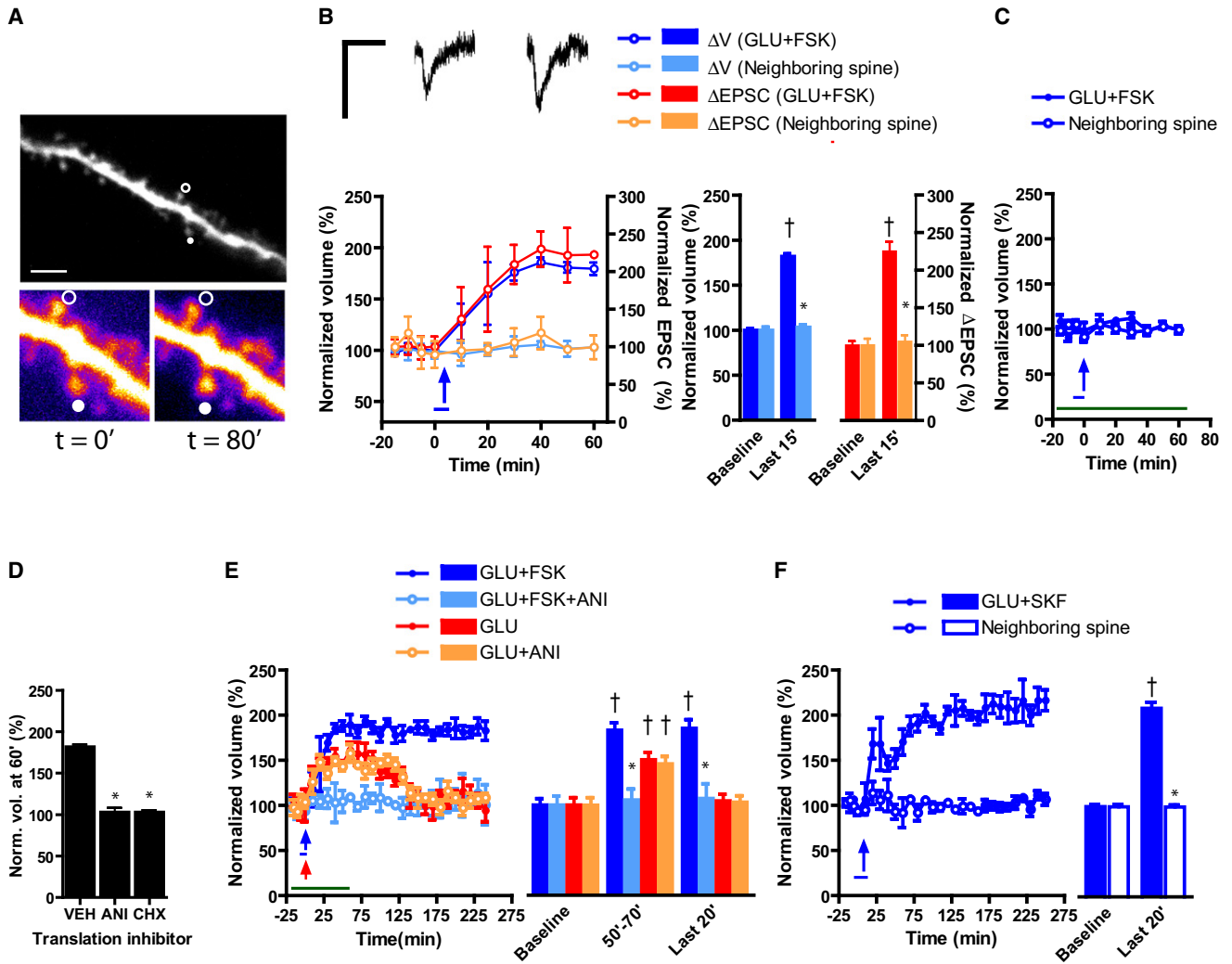
Figure 1. L-LTP and E-LTP Could Be Induced at Single Spines

(A) Example of tetanized spine (filled circle), and neighboring spine (open circle) before (t = 0′) and 80′ after GLU+FSK stimulation.

(B) Pooled data from four spines show concomitant increase of spine volume and uEPSC strength of the stimulated, but not neighboring, spine.

(C and D) Pooled data from five experiments each show that anisomycin or cycloheximide treatment during the experiment abolished spine growth.

(E) E-LTP, induced by GLU stimulation, was shorter lasting than L-LTP and was insensitive to anisomycin (eight experiments each). Anisomycin was applied only during the experiments indicated with the open circles.

(F) Pooled data from five spines show an increase in spine volume with GLU+SKF stimulation. Blue and green bars represent forskolin (SKF38393 in F) and anisomycin, respectively. Blue and red arrows represent uncaging tetani. *p < 0.01 between adjacent bars; †p < 0.001 in comparison with corresponding baseline. GLU, tetanus of glutamate uncaging (30 pulses of 4 ms each at 0.5 Hz) at single spine; this is used in Figures 1–5, FSK, forskolin (bath applied); VEH, vehicle; ANI, anisomycin; CHX, cycloheximide; SKF, SKF38393. Scale bar represents 10 μm. Electrophysiological trace scale bar represents 10 ms and 15 pA. Normalization performed as percentage of average baseline value for each spine. All data are mean ± SEM.

many hours, we relied on a different technique. We gave single uncaging pulses to spines of different sizes and measured the postsynaptic response of the spines, namely the uEPSC amplitude, by whole-cell patch electrophysiology (voltage-clamp) and compared that with the volume of the spine head. We found, in agreement with published data (Asrican et al., 2007; Matsuzaki et al., 2004; Smith et al., 2003), that the uEPSC amplitude measured at a spine was directly proportional to its volume (Figures S3A–S3E). Because this relationship held across cells within a slice (Figures S3B–S3E) (Smith et al., 2003), the initial

postsynaptic strength of a spine is calculable from a spine volume-to-uEPSC amplitude calibration function obtained from a different cell within the slice. Thus, we recorded the uEPSC amplitude of different spines along a dendritic branch from a cell (cell 1) that neighbored the cell of interest (cell 2) to determine a spine volume-to-uEPSC amplitude calibration function. We then induced STC at cell 2 by stimulating two spines, L1 (GLU+FSK stimulation) and L2 (GLU+FSK stimulation in the presence of anisomycin), on an analogous branch in cell 2 and followed this with whole-cell recordings and single-spine
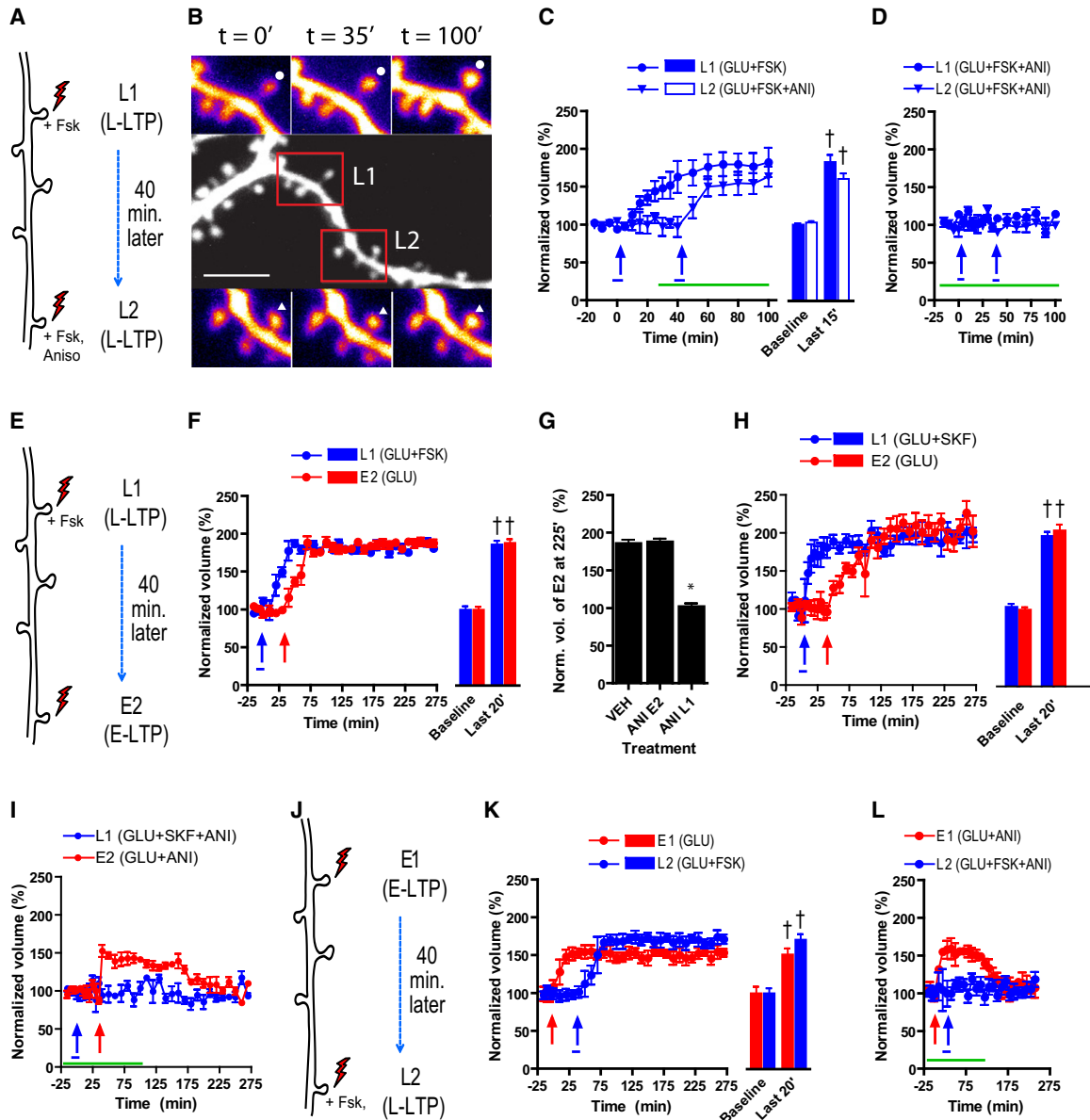
Figure 2. STC Occurred at Single Spines

(A) Schematic of STC experiment using GLU+FSK stimulation at two spines, the second in the presence of anisomycin (L1, L2).

(B) Example of L1, L2 spines before L1 stimulation (t = 0′), L2 stimulation (t = 35′), and at end of experiment (t = 100′) demonstrating STC.

(C) Pooled data from eight experiments show STC at L2.

(D) STC was abolished by anisomycin applied during L1 and L2 stimulations (five experiments).

(E) Schematic of STC using GLU stimulation at spine 2 (E2) after GLU+FSK stimulation at spine 1 (L1).

(F) Pooled data from six experiments show STC at E2.

(G) STC at E2 was sensitive to anisomycin present during L1 stimulation, but not E2 stimulation (five experiments).

(H) Pooled data from five experiments show that STC occurred at E2 when L1 was given GLU+SKF stimulation.

(I) Anisomycin present during GLU+SKF stimulation of L1 blocked L-LTP at both L1 and E2 (five experiments).

(J) Schematic of STC using GLU stimulation (E1) before GLU+FSK stimulation (L2).

(K) Pooled data from seven experiments show STC at E1.

(L) STC at E1 was sensitive to anisomycin present during L2 stimulation (five experiments). Blue and red arrows represent uncaging tetanus. Blue and green bars represent forskolin (SKF38393 in H and I) and anisomycin, respectively.

*p < 0.01 between adjacent bars; †p < 0.001 in comparison with corresponding baseline. GLU, tetanus of glutamate uncaging; FSK, forskolin (bath applied); VEH, vehicle; ANI, anisomycin; CHX, cycloheximide; SKF, SKF38393. Scale bar represents 10 μm. Normalization performed as percentage of average baseline value for each spine. All data are mean ± SEM.

stimulations of L1 and L2 and neighboring spines from cell 2 at the end of the experiment to determine the stimulated and neighboring spines' strengths. We estimated the potentiation of L1 and L2 by normalizing the final uEPSC amplitude to the initial uEPSC amplitude estimated from the initial spine volume of L1 and L2 using the previously calculated calibration function from cell 1. We found that both L1 and L2 underwent potentiation (Table 1; Figures S3F and S3G), whereas there was no change in neighboring spines, both in terms of volume and estimated uEPSC amplitude. Combining these data with the data from Figure 1B; Figures S1B–S1D and data from the literature (Tanaka et al., 2008), we conclude that similar to the case for E-LTP (Asrican et al., 2007; Harvey and Svoboda, 2007; Matsuzaki et al., 2004), the spine volume increases that we observed at the spines to which the GLU+FSK stimulation was given and also at the spines in which STC occurred are indicative of a change in potentiation. Thus, we used spine volume change as a measure of both L-LTP and E-LTP for the remainder of the experiments.

Analogously to data obtained from a population of synapses using field recordings and stimulation (Frey and Morris, 1997), we found that GLU+FSK stimulation at one spine (L1) followed by GLU stimulation (which normally induces only E-LTP) at a second spine (E2; Figure 2E) resulted in L-LTP expression not only at L1 but also at E2, again demonstrating STC in our single-spine stimulation system (Figure 2F; Figure S2A). This effect was not caused by residual effects of forskolin from the L1 stimulation as there was no L-LTP expressed at E2 when uncaging pulses were not given at L1 (Figure S4A). This increase was independent of protein synthesis in response to E2 stimulation but was dependent on protein synthesis in response to L1 stimulation (Figure 2G). Similar data were also obtained when L1 was given GLU+SKF stimulation instead of GLU+FSK stimulation (Figures 2H and 2I). In addition, using our uEPSC-potentiation estimation method mentioned above, we found that this change in spine volume at E2 was accompanied by an increase in synaptic strength (Table 1; Figures S3F and S3G). Analogous to STC measured at a population level (Frey and Morris, 1998), STC at the single-spine level is temporally bidirectional as GLU stimulation given to one spine (E1) prior to GLU+FSK stimulation given to a second spine (L2; Figure 2J) resulted in the expression of L-LTP at both spines (Figure 2K). This expression of L-LTP required protein synthesis at L2 (Figure 2L).

The Temporal Bidirectionality of STC Is Asymmetric
An important component of STC is that both the synaptic tag and the rate-limiting PrP(s) have limited lifetimes (Frey and Morris, 1997, 1998). However, it has not been determined how different the two lifetimes are, a crucial point in understanding the dynamics of the temporal bidirectionality of STC. To determine the lifetime of the rate-limiting PrP, we applied GLU+FSK stimulation to two spines (L1, L2) with anisomycin present only during L2 stimulation and varied the time between L1 and L2 stimulations. The efficiency of STC at L2, which would be proportional to the concentration of the rate-limiting PrP (Frey and Morris, 1997), was inversely related to the time between L1 and L2 stimulations (Figure 3A), with STC taking place only if L2 was stimulated within 90 min of L1 stimulation. These data suggest that the rate-limiting PrP decayed within 90 min. We obtained a similar

Table 1. Spines that Grew Also Showed Increased uEPSC Amplitudes

ΔVol (%)	ΔuEPSC (%)	Neighbor ΔVol (%)	Neighbor ΔuEPSC (%)	Stimulation Type
177	296	95	92	L-LTP (60′)
195	278	94	109	L-LTP (60′)
156[a]	170	101	98	L1 (100′)
167[a]	178	101	98	L2 (100′)
164[b]	181	95	93	L1 (100′)
183[b]	197	95	93	L2 (100′)
189[c]	193	100	94	L1 (100′)
155[c]	179	100	94	L2 (100′)
102	98	104	102	E-LTP (270′)
93	116	97	98	E-LTP (270′)
97	107	107	110	E-LTP (270′)
199[d]	197	103	113	L1 (270′)
233[d]	249	103	113	E2 (270′)
187[e]	229	107	102	L1 (270′)
231[e]	298	107	102	E2 (270′)
203[f]	238	107	105	L1 (270′)
195[f]	205	107	105	E2 (270′)

Data from 17 stimulated spines demonstrate that spines that increased in volume also had an increase in uEPSC strength. The percent (%) uEPSC change was determined by normalizing the final uEPSC to the estimated initial uEPSC as described in the text (see sixth paragraph under the L-LTP and STC Can Be Induced and Monitored at the Single-Spine Level section). Each pair of rows marked [a] through [f] indicates two different stimulated spines from the same experiment. Data also plotted as Figures S3F and S3G.

time course of STC when we replaced GLU+FSK stimulation at L2 with GLU stimulation without anisomycin (E2; Figure 3B). To determine the lifetime of the synaptic tag, we gave GLU stimulation to one spine (E1) before giving GLU+FSK stimulation to a second spine (L2), varying the time between E1 and L2 stimulations. We found that STC efficiency, which is thought to be a measure of the tag strength (Frey and Morris, 1998), was also inversely related to the temporal interval between E1 and L2 stimulations, with STC occurring fully at an interval of 90 min but being abolished at an interval of 3 hr (Figure 3C). Thus, the temporal bidirectionality of STC is asymmetric as the lifetime of the tag (approximately 120 min, Figure 3C) is different from the lifetime of the rate-limiting PrP (approximately 90 min, Figures 3A and 3B). These data suggest that the temporal order in which information arrives at a dendrite is important in determining how it is consolidated as part of a stable engram.

The ability to induce and observe STC at the single-spine level also allowed us to relate the magnitude of E-LTP expression at a single spine to the strength of the synaptic tag. This was not possible with field recordings and stimulations that measure the average response of a population of synapses. We found that there was a strong correlation between the strength of E-LTP expression (measured as E1 volume just prior to L2 stimulation) and the strength of the synaptic tag (measured as the volume of E1 3 hr after L2 stimulation thought to be proportional
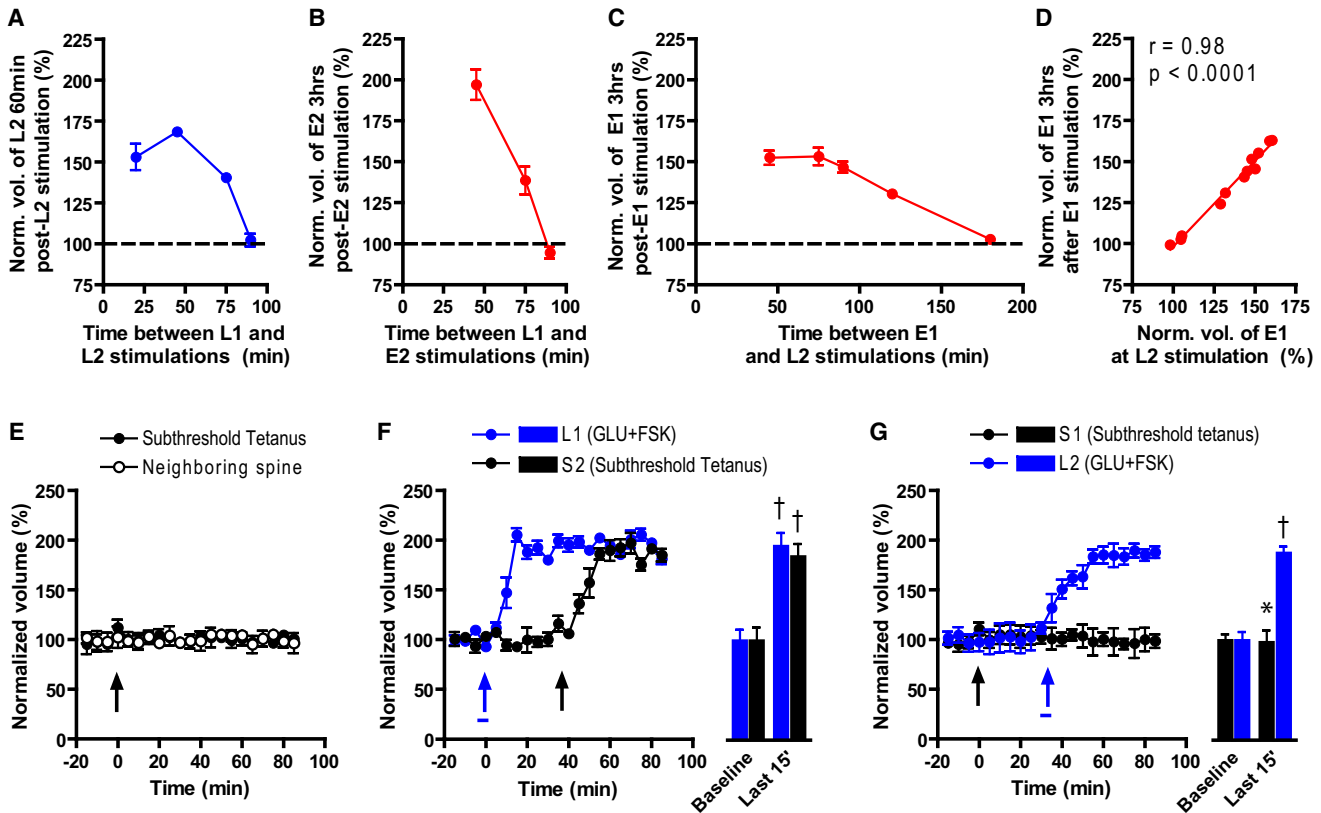
Figure 3. The Temporal Bidirectionality of STC Was Asymmetric

(A and B) Varying the time between L1 (GLU+FSK stimulation) and L2 (GLU+FSK stimulation with anisomycin) stimulations (A) or L1 (GLU+FSK stimulation) and E2 (GLU stimulation) stimulations (B) demonstrates that the lifetime of the rate-limiting PrP, measured by STC efficiency at L2 (A) or E2 (B), was less than 90 min (A and B: both $p < 0.001$; $n = 3$ for each time point).

(C) Varying the time between E1 (GLU stimulation) and L2 (GLU+FSK stimulation) stimulations showed that the lifetime of the synaptic tag, measured by STC efficiency at E1, was longer than 90 min and less than 180 min ($p < 0.001$; $n = 3$ for each experiment).

(D) Strong correlation between the volume of E1 prior to L2 stimulation and E1 at end of experiment demonstrates that L-LTP induction or expression stabilized prior induced E-LTP expression without changing its magnitude.

(E) Subthreshold stimulation had no effect on spine volume (six experiments).

(F) GLU+FSK stimulation at one spine (L1) resulted in STC at second spine (S2) given subthreshold stimulation later (six experiments).

(G) GLU+FSK stimulation at one spine (L2) did not result in STC at second spine (S1) given subthreshold stimulation earlier (six experiments). Black and blue arrows represent subthreshold (1 ms) and normal (4 ms) uncaging tetani, respectively. Blue bar represents forskolin.

*$p < 0.01$ between adjacent bars; †$p < 0.001$ in comparison with corresponding baseline. GLU, tetanus of glutamate uncaging; FSK, forskolin (bath applied). Normalization performed as percentage of average baseline value for each spine. All data are mean ± SEM.

to the synaptic tag strength; Figure 3D). This indicates that the strength of the synaptic tag is tightly correlated with the level of E-LTP expression when GLU stimulation precedes GLU+FSK stimulation. Under these conditions, the magnitudes of L-LTP at the spines given GLU stimulation were generally lower than that at spines given GLU+FSK stimulation (Figure 2K). On the other hand, when GLU stimulation followed GLU+FSK stimulation, the magnitude of L-LTP at the spine given GLU stimulation (E2) tended to be similar to that of the spine given GLU+FSK stimulation (Figure 2F).

Therefore, we hypothesized that PrPs strengthen tags at spines stimulated later, but not earlier. To test this idea, we employed a subthreshold stimulus (each uncaging laser pulse lasts 1 ms instead of 4 ms) that, consistent with previously reported data (Harvey and Svoboda, 2007), did not cause a change

in spine volume (Figure 3E). When this stimulus was given to a spine (S2) after GLU+FSK stimulation was given to another spine (L1), a significant increase in spine volume was seen at both L1 and S2 (Figure 3F). Similar to the L1-L2 stimulation (Figures 2C and 2D) and L1-E2 stimulation (Figure 2F) experiments, this growth depended on protein synthesis during L1 stimulation, but not S2 stimulation (data not shown). However, when the same subthreshold stimulus (S1) was given to one spine before GLU+FSK stimulation was given to a second spine (L2), no growth at S1 was seen, whereas L2 grew normally (Figure 3G). These data support the hypothesis that PrPs strengthen tags at spines stimulated after their production, but not those stimulated earlier. Thus, though STC is temporally bidirectional, the two directions are different, not only because the lifetimes of the synaptic tag and the rate-limiting PrP are different, but also
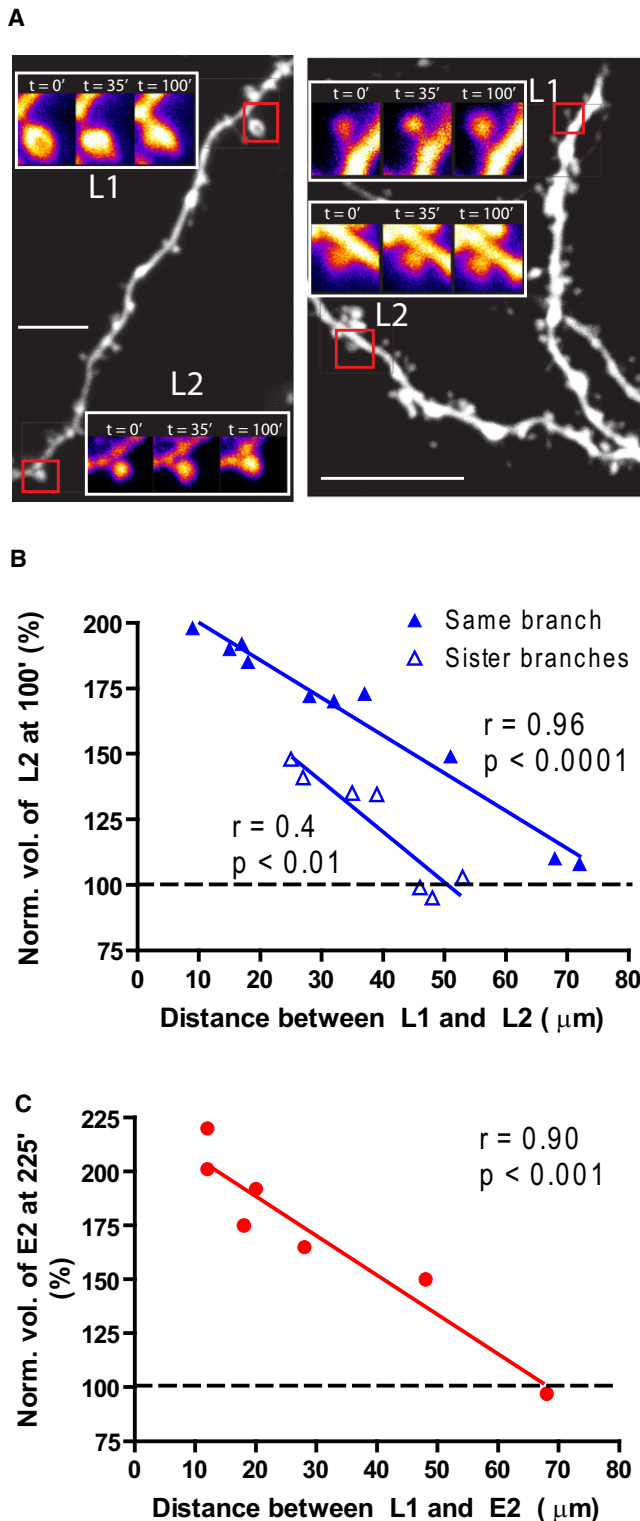
A

B

C

because L-LTP induction or expression seems to facilitate tag formation at spines stimulated later, but not at spines stimulated earlier.

Spatial Localization and Dendritic Branch Bias of STC Support the CPH

Having established STC at the single-spine level and revealed its asymmetric bidirectionality, we next examined the spatial span over which STC occurs, an issue central to the CPH (Govindarajan et al., 2006). The spatial relationship between spines participating in STC cannot be studied using field stimulation, since it results in the activation of many unidentified spines. But, it can be studied in our system by varying the distance between two spines both of which are given GLU+FSK stimulations (L1, L2) with only L2 stimulation conducted in the presence of anisomycin. This allowed us to determine if there is a limit on the distance over which STC can occur. We found that the efficiency of STC was inversely proportional to distance and that STC was barely detectable when the distance between the two stimulated spines became as large as 70 μm (Figures 4A and 4B). The same result was obtained when GLU+FSK stimulation with anisomycin at L2 was replaced with GLU stimulation without anisomycin (E2; Figure 4C).

We next repeated the same experiment but moved L2 to a sister branch. L1 and L2 were always on tertiary dendrites, and time between stimulations was kept constant at 45 min. We found that the efficiency of STC was considerably reduced in this configuration of stimulated spine pairs and that no STC was seen when the distance between L1 and L2 was at 50 μm or greater (Figures 4A and 4B). This, along with the data above from two spines on the same branch, indicates that STC is likely to be a local process operating preferentially at the level of a dendritic branch, as predicted by the CPH (Govindarajan et al., 2006). This bias toward STC occurring more efficiently on a single branch could occur either passively due to dilution of the newly synthesized proteins at the branch point or via some specific biochemical mechanism present at branch points.

Competition for STC Expression Also Supports the CPH

If PrPs are available within a limited dendritic compartment for a limited time, would the stimulation of multiple inputs within a short distance and time result in competition for limiting PrPs? Indeed, the CPH also predicts that competition among stimulated synapses for limiting PrPs would further cause memory engrams to be stored in a spatially clustered fashion, as the limiting PrPs would be used up by spines close to the translation site (Govindarajan et al., 2006). It has previously been

GLU+FSK stimulation. L2 was stimulated at 45 min in the presence of anisomycin.
(B) Quantification of several experiments demonstrates that the efficiency of STC decreased with increasing distance and with stimulated spines being on different branches. (C) Replacing L2 with GLU stimulation confirmed that STC efficiency decreased with increasing distance between stimulated spines. Scale bar represents 10 μm. Normalization performed as percentage of average baseline value for each spine. All data are mean ± SEM.

Figure 4. The Spatial Localization of STC Demonstrated the CPH
(A) Left panel shows example of two spines stimulated on the same branch 50 μm apart (measured along the dendrite), whereas the right panel shows an example of two stimulated spines 48 μm apart (measured along the dendrite) on adjacent branches. In both cases the spines (L1, L2) were given

shown using the field stimulation and field recording methods that different inputs can compete for PrPs when the protein pool was made limited (Fonseca et al., 2004) by the application of a translation inhibitor. However, it remains to be determined whether the protein pool would indeed be limiting under more physiological conditions (i.e., in the absence of the translation inhibitor). We also wanted to use our single-spine methodology to examine the temporal dynamics of individual spine changes during situations in which multiply stimulated spines might compete for limiting PrPs. For these purposes, we stimulated two spines between 10 and 20 μm apart on the same branch (labeled L1 and L2) 1 min apart with GLU+FSK stimulation, with the intention of increasing the number of stimulated spines until L-LTP expression was inhibited. We found that stimulating only two spines already caused both spines to reach their maximum volume slower as compared to stimulating only one spine (Figure 5A compared to Figure 1B and Figures S1A, and S1B, quantified in Figure 5B). Analyzing the temporal dynamics of the competing spines, we found that during the first 30 min, there was a large correlated fluctuation during the poststimulation period in the volumes of L1 and L2, such that the growth of one was accompanied by a shrinking of the other (examples shown in Figure 5C and Figures S4B–S4D, quantified in Figure 5D). In contrast, there was no significant correlation during the baseline period and during time points 40 min or longer after stimulation. In addition, there was also no correlation between stimulated spines and unstimulated neighboring spines (Figure 5E) indicating that the competition is specific to stimulated spines. These data suggest that the amount of protein that can be produced within a dendritic compartment at a certain time is limited such that two spines stimulated close together in space and time may compete for available proteins and, hence, for the expression of L-LTP. This might occur due to the relatively limited translational machinery and/or mRNA at the dendritic branch (as compared to the soma) (Schuman et al., 2006). Activity-induced mRNA degradation may also contribute to this phenomenon (Giorgi et al., 2007). These results also suggest that spine growth is a bidirectional rather than a unidirectional dynamic process.

Can later stimulated spines still compete with earlier stimulated spines? To address this question, we gave GLU stimulation to a third spine (E3), 5–15 μm from L1 and L2 spatially located between L1 and L2, 30 min later, at a time when both L1 and L2 have grown, but not to their maximal levels. We found that the growth of L1 and L2 was slowed down by the stimulation of E3 (Figures 5F and 5G), and the growth of E3 was reduced by the previous stimulation of L1 and L2, as compared to the case of E2 when only L1 was previously stimulated (Figures 5F and 5H). A similar result was obtained when GLU stimulation at E3 was replaced with GLU+FSK stimulation with anisomycin (L3; Figures S4E–S4G). Thus, we demonstrate that at the single-spine level, spines can compete with each other for the expression of L-LTP, presumably due to competition for PrPs.

Dendritic Branch Bias of L-LTP Induction

The NMDA glutamate receptor (NMDAR), necessary for the induction of many forms of synaptic plasticity, can only be acti-

vated when it is not blocked by Mg^{+2} ions (Malenka and Bear, 2004). This unblocking of the receptor is thought to occur in vivo through depolarization caused by the cooperative activation of multiple AMPA glutamate receptors (Malenka and Bear, 2004). In our experiments described up to this point, we used 0 mM Mg^{+2} during the uncaging process to allow NMDAR activation without stimulating more than one spine. Thus, we were able to study STC without the confound of L-LTP being induced at multiple spines. However, under physiological conditions, the concentration of Mg^{+2} is 0.8–1.2 mM (Chutkow, 1974). In a bid to simulate such conditions, we sought to establish a protocol that would allow for LTP induction in the presence of 1 mM Mg^{+2} by stimulating multiple spines in a pseudosynchronous manner (Losonczy and Magee, 2006; Losonczy et al., 2008). This method used a higher concentration of MNI-Glutamate (10 mM) and a shorter pulse (0.1 ms) to allow for rapid activation of multiple spines. We first confirmed that L-LTP, E-LTP, and STC could be induced by this method of glutamate uncaging applied at 0 mM Mg^{+2} using the single-spine stimulation protocol (Figures S5A–S5C).

We then attempted to induce L-LTP by pseudosynchronous (<6 ms) stimulation of multiple spines within a single oblique tertiary apical dendritic branch (Losonczy and Magee, 2006; Losonczy et al., 2008) in ACSF containing 1 mM Mg^{+2}, 2 mM Ca^{+2}, and 100 μM of the D1R agonist SKF38393 (GLU+SKF stimulation). For technical reasons, the spines had to be on the same z plane and within ~20 μm of each other. Since it is not known how many spines need to be stimulated for L-LTP to be induced in this manner, different numbers of spines were stimulated in different experiments. When we compiled a frequency distribution of normalized spine volumes across all the experiments, we found that the distribution of spine volumes poststimulation was described by a bimodal distribution (Figure S5D). The majority of data points were part of a mode that was indistinguishable from the distribution of spine volumes resulting from fluctuations seen during the baseline period. However, there were some data points that were part of a second mode with a higher normalized volume (Figure S5D). We defined these as potentiated spines and discovered that these data points resulted from a small proportion of stimulated spines that underwent a significant increase in volume (e.g., insets in Figure 6A, quantified in Figures 6B and 6C). We also quantified the number of potentiated spines as a function of number of stimulated spines and determined that when 12 or more spines were stimulated, a small proportion of the stimulated spines were potentiated, whereas when ten or fewer spines were stimulated, no spines were potentiated (Figure 6D). This potentiation was dependent on protein synthesis as it was abolished when the spines were stimulated in the presence of anisomycin (Figure S5E). Unstimulated spines were never potentiated (data not shown).

We repeated the experiment, but this time split the stimulated spines across two sister tertiary apical oblique branches (e.g., in Figure 6E). Under these conditions, we were unable to induce a spine volume change at any spine (Figure 6F). Thus, in addition to STC, the formation of L-LTP itself is biased toward occurring more on a single dendritic branch, further supporting the CPH.
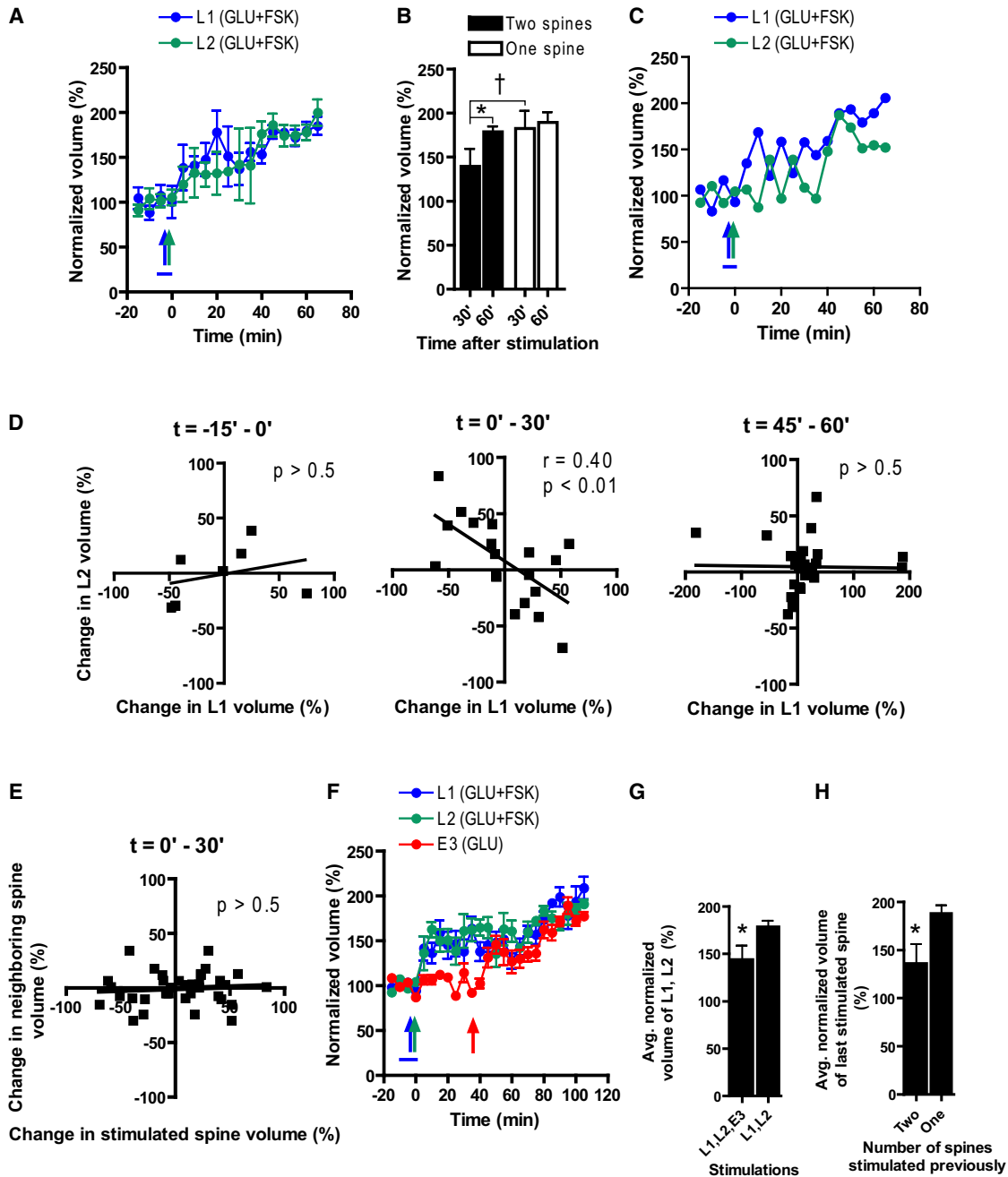
Figure 5. Competition between Spines

(A) Pooled data from seven experiments show that stimulating two spines (10–20 μm apart; L1, L2; GLU+FSK stimulation) 1 min apart resulted in slower growth of both spines compared to stimulating one spine (GLU+FSK stimulation).

(B) Spine growth was compared between two cases when either a single spine was stimulated (Figures 1B and S1A) or two spines 10–20 μm apart were stimulated successively.

(C) Representative experiment showing complementary growth and shrinkage during the first 30 min, but not after 35 min, poststimulation.

(D) Correlation of the change in spine volume at L1 with the change in spine volume at L2 at each 5-min interval shows that L1 and L2 grew independently prior to stimulation, and after 35 min poststimulation. However, within the first 30 min after stimulation, one spine grew at the expense of the other. Each time point on the graph represents the difference in volume between two successive time points using spines from six independent experiments.

(E) In contrast to (D) there was no correlation between stimulated spines and their neighbors during the 0- to 30-min period, indicating that the competition was specific to stimulated spines.

(F) Pooled data from six experiments show that a third spine stimulated with GLU stimulation (E3) could compete for growth with spines given GLU+FSK stimulation earlier (L1, L2).
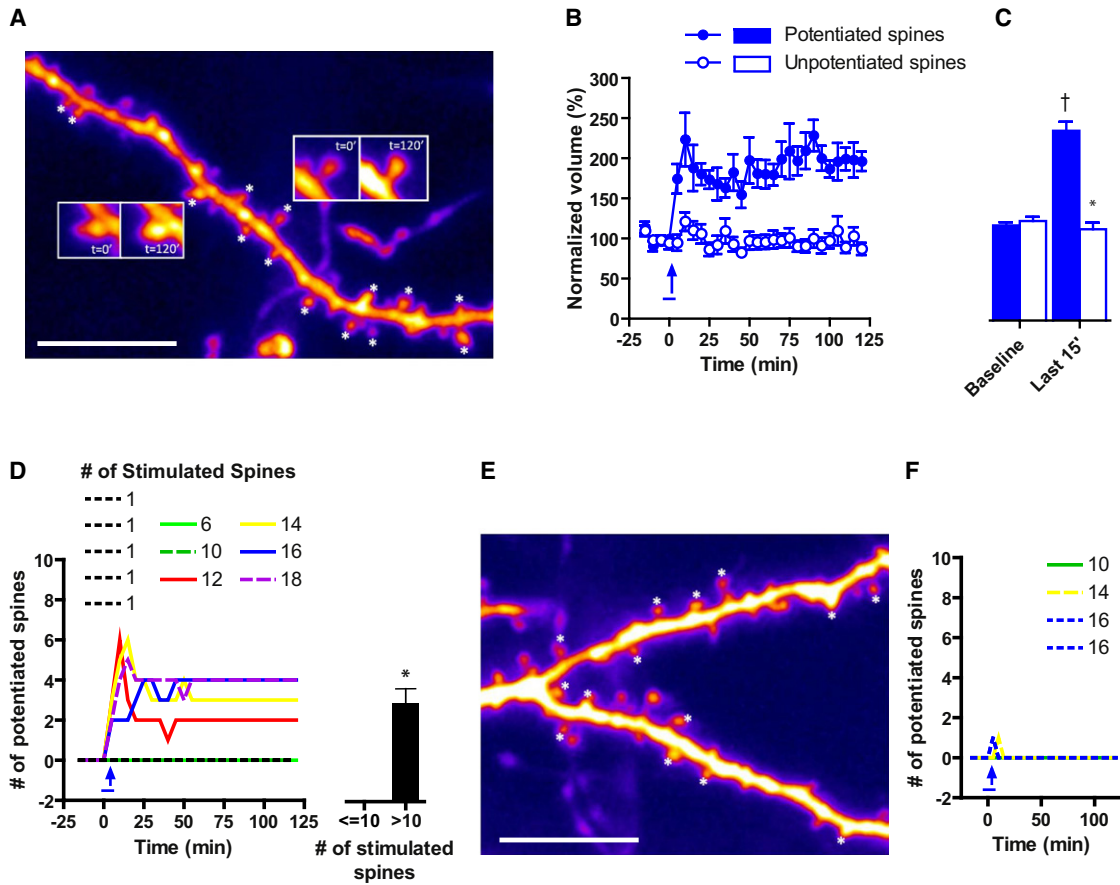
Figure 6. L-LTP Induced by Stimulation of Multiple Spines

(A) Example of branch with 14 stimulated spines (marked with *). Insets contain examples of a spine that was potentiated (right) and one that was not (left).

(B and C) Pooled data from 81 spines demonstrate the differences between the potentiated spines (13 spines) and unpotentiated spines (68 spines). Potentiated spines were defined as those that were part of the larger mode in the bimodal distribution of spine volumes shown in Figure S5D and described in the text.

(D) Pooled data from 81 spines show the number of spines that were potentiated as a function of time. Each data set is a single experiment, whose legend indicates the number of spines stimulated during that experiment. Thus, when less than ten spines were stimulated, no spines were potentiated.

(E) Example with 14 stimulated spines (marked with *) across two sister branches.

(F) Pooled data from 56 spines show that no spines were potentiated when the stimulated spines were split across a branch. Each data set is a single experiment, whose legend indicates the number of spines stimulated during that experiment. Blue bar indicates time of SKF38393 addition (for 5 min), and blue arrow indicates time of uncaging tetanus (100 pulses for 0.1 ms each at 2 Hz [denoted GLU in Figures 6 and 7]). Tetanus applied such that for each "pulse" of the tetanus, all spines were stimulated in <6 ms.

†$p < 0.05$ between stimulated condition and baseline condition; *$p < 0.05$ between potentiated and unpotentiated state (B) or between ten or less and more than ten spines (D). Scale bar represents 5 μm. Normalization performed as percentage of average baseline value for each spine. All data are mean ± SEM.

L-LTP, E-LTP, and STC with Multispine Stimulation

We then compared the expression of L-LTP and E-LTP induced by multispine stimulation. In these experiments, 14 spines were activated either by GLU+SKF stimulation (for L-LTP induction) or GLU stimulation (for E-LTP induction). We found that in both cases, the spines could be split into two populations—those that were potentiated, and those that were not (Figures 7A–7C). As expected, the volume of the spines expressing E-LTP declined to baseline within 3 hr (Figures 7B–7D), whereas the volume of the spines expressing L-LTP remained elevated

(G) Stimulation of E3 slowed growth of L1, L2, quantified by comparing the average growth of L1 and L2 30 min after E3 is stimulated with the average growth of L1 and L2 in the absence of E3 stimulation (from Figure 3D).

(H) Stimulating two spines with GLU+FSK stimulation prior to later GLU stimulation (E3 after L1, L2) reduced the efficiency of the later stimulation, as compared to stimulating only one spine prior to the later stimulation (E2 after only L1 from Figure 1L). Blue, teal, and red arrows represent uncaging tetani. Blue bar represents forskolin.

*$p < 0.01$ between adjacent bar; †$p < 0.05$ in Figure 5B in comparison between one and two spines for the 30′ time point. GLU, tetanus of glutamate uncaging; FSK, forskolin (bath applied). Normalization performed as percentage of average baseline value for each spine. All data are mean ± SEM.
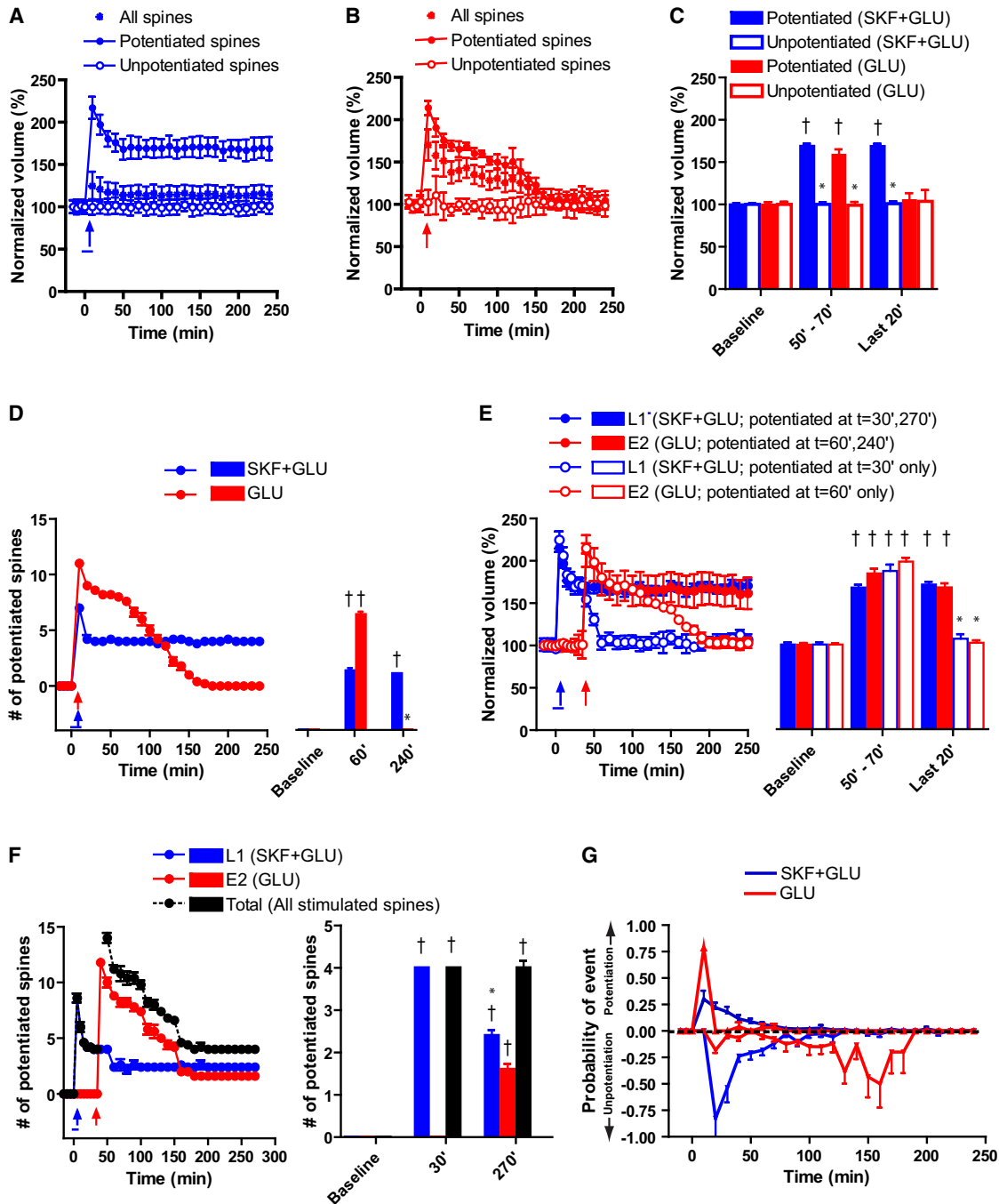
Figure 7. L-LTP, E-LTP, and STC Induced by Stimulation of Multiple Spines

(A) Pooled data from five experiments, each with 14 spines stimulated on a single branch, show that bath application of the D1R agonist SKF38393 along with pseudosynchronous stimulation of 14 spines resulted in a robust difference in spine volume between potentiated and unpotentiated spines. The increased spine volume lasted throughout the experiment.

(B) Pooled data from five experiments, each with 14 spines stimulated on a single branch, show that pseudosynchronous stimulation of 14 spines resulted in a robust difference in spine volume between potentiated and unpotentiated spines. However, the potentiated spines' volume returned to baseline within 3 hr.

(C) Quantification of the data from (A) and (B) show that the increased spine volume was statistically significant.

(D) Pooled data from five experiments show that the number of spines that underwent L-LTP was less than the number of spines that underwent E-LTP in our conditions.

(E) When SKF38393 was bath applied along with pseudosynchronous stimulation of 14 spines (L1), followed 40 min later by pseudosynchronous stimulation of another set of 14 spines (E2), four populations of potentiated spines were seen (unpotentiated spines are not shown in the graph for clarity). Some L1 spines (blue solid circles) were potentiated throughout the experiments, whereas some L1 spines (blue open circles) that were potentiated just prior to E2 stimulation returned to baseline shortly afterward. Among spines that were potentiated as a result of E2 stimulation, there were also two groups. Most of the spines (red open spines) returned to baseline, but

throughout the experiment (Figures 7A, 7C, and 7D). Interestingly, the proportion of spines that expressed E-LTP was higher than the proportion of spines that expressed L-LTP (Figure 7D).

When one set of 14 spines received GLU stimulations (E2s) 40 min after another set of 14 spines was given GLU+SKF stimulations (L1s), we found evidence of STC. As shown in Figures 7E and 7F, there was a subpopulation of spines among the E2 set that had an elevated increase in spine volume throughout the experiment (STC; Figure 7E, filled red circles, and Figure 7F, filled red bars). Thus, in a manner similar to our previous experiments conducted using the single-spine stimulation protocol in 0 mM Mg^{+2}, L-LTP, E-LTP, and STC can all be induced by the cooperative activation of multiple spines under physiological Mg^{+2} conditions.

When we examined the set of spines (L1s) that had received GLU+FSK stimulations, we noticed that there was a subpopulation of spines that were potentiated prior to GLU stimulations at E2 spines but whose volume returned to baseline shortly after the GLU stimulations were given (Figure 7E, open blue circles). These data were supported by a quantification of the number of spines potentiated in these experiments. As Figure 7F shows, the stimulation of E2 led to a reduction in the number of potentiated L1 spines, concomitant with a set of E2 spines that now expressed LTP throughout the rest of the experiment. Interestingly, the total number of spines potentiated just prior to E2 stimulation is statistically indistinguishable from the total number of spines potentiated at the end of the experiment. This supports our model whereby spines at which E-LTP is induced can compete with spines at which L-LTP has been induced, which in turn further bolsters the CPH.

Further evidence for competition during L-LTP expression was obtained by a detailed examination of individual spine dynamics (examples shown in Figures S5F–S5H) during the expression of L-LTP and E-LTP. We examined the probability of transitions from the unpotentiated state to the potentiated state and discovered that during the first 60 min after L-LTP induction, a number of spines transitioned from the unpotentiated state to the potentiated state (Figure 7G, top half, blue line). This was balanced by an approximately equal number of spines making the opposite transition (Figure 7G, bottom half, blue line) leading to a constant number of potentiated spines (Figures 6D and 7D). In contrast, following E-LTP induction, there was an initial burst of potentiation (Figure 7G, top half, red line), followed by a period of 120 min over which spine volumes were stable, in turn followed by an unpotentiated period lasting from 120 to 180 min (Figure 7G, bottom half, red line). Thus, our data point toward competition among spines for L-LTP but not for E-LTP expression.

DISCUSSION

We have demonstrated using single-synapse stimulation in the absence of Mg^{+2} that the temporal bidirectionality of L-LTP facilitation is asymmetric, that STC is a spatially localized process favoring a dendritic branch, and that the PrP pool is limiting, resulting in competition among stimulated spines for expression of L-LTP. This competition was also observed when we induced L-LTP under 1 mM Mg^{+2} conditions using multispine stimulation. Additionally, we found that only a fraction (approximately 25%) of stimulated spines expressed L-LTP. These data suggest that the amount of protein produced by such stimuli is limiting, and thus, the temporal and spatial constraints of STC that we discovered are likely to be similar between the cases where L-LTP was induced by single-spine stimulation and where it was induced by multiple spine stimulation.

Synapses that participate in a long-term memory engram will arise not only from spines at which L-LTP was induced but also from spines at which E-LTP was originally induced via STC. However, it is essential that the spines at which E-LTP was induced be in close spatial proximity to the spines at which L-LTP was induced, preferably within the same dendritic branch. The branch bias of L-LTP induction found in our multispine stimulation experiments conducted under 1 mM Mg^{+2} conditions implies that L-LTP induction will preferentially occur within distinct dendritic branches, and not throughout the dendritic arbor. These dendritic branch biases for the induction and expression of L-LTP would result in a preferential spatial clustering within dendritic branches of synapses that would participate in a long-term memory engram. This clustering effect would be enhanced by the competitive nature of L-LTP induction and STC, as capture of protein by synapses near the location of the L-LTP induction would result in less protein available to synapses farther away. If L-LTP induction requires the participating synapses to be within a limited dendritic distance within the branch, a hypothesis that we were unable to test for technical reasons, then it remains possible that the integrative unit for a long-term memory engram is a subregion of a dendritic branch, and not the entire branch.

These data suggest that at the single-cell level, hippocampal CA1 cells store long-term memory engrams at synapses that tend to be clustered within dendritic branches as opposed to dispersed throughout the dendritic arbor (Govindarajan et al., 2006). Storing long-term memory engrams in a clustered fashion has advantages over storing them in a dispersed fashion because it would facilitate the formation of memories and increase the ability for memories to be recalled, due to the ability of synaptic inputs arriving at a branch to supralinearly summate

some (red solid circles) stayed potentiated throughout the rest of the experiment.

(F) Pooled data from five experiments showing the number of spines that belong to the four groups in (D). Note that there was a statistical difference between the number of L1 spines potentiated at 30′ versus 270′ and that the number of E2 spines potentiated at 270′ is significantly different than zero. Also, there was no statistical difference between the total number of spines potentiated at 30′ and at 270′.

(G) Plot of probability of spines transitioning from unpotentiated state to potentiated state (top half) and vice versa (bottom half). In the case of E-LTP, there was an initial burst of potentiation at 5 min, followed by an unpotentiated period from 120 to 180 min. In the case of L-LTP, both potentiation and an unpotentiated state occurred at significant amounts throughout the first 60 min after stimulation. Because the number of potentiated spines was constant (D), this supports the case for competition among spines. Blue bar indicates time of SKF38393 addition (for 5 min), and blue, red arrows indicate time of uncaging tetanus. †p < 0.05 between later time points and baseline conditions; *p < 0.05 between potentiated and unpotentiated state (C), between 60 and 240 min (D), or between 30 and 270 min (F). SKF, SKF38393; GLU, tetanus of glutamate uncaging. Normalization performed as percentage of average baseline value for each spine. All data are mean ± SEM.

in depolarizing the cell (Gasparini and Magee, 2006; Gasparini et al., 2004; Govindarajan et al., 2006; Poirazi et al., 2003a, 2003b; Poirazi and Mel, 2001). In addition, this supralinear summation (Gasparini and Magee, 2006; Gasparini et al., 2004; Poirazi et al., 2003a; Poirazi and Mel, 2001) ensures that the same number of synaptic inputs will have different effects depending on whether they are on the same branch or not, leading to an increase in the number of patterns that a neuron could encode without interference (Govindarajan et al., 2006; Poirazi and Mel, 2001).

The constraints on STC are clearly different from the constraints on the facilitation of E-LTP (crosstalk) (Harvey and Svoboda, 2007; Harvey et al., 2008), in that STC is protein synthesis dependent, whereas crosstalk is not, it can operate over a larger time window (90 min versus 10 min for crosstalk) and over a larger distance (70 μm versus 10 μm for crosstalk), and it occurs both if E-LTP is induced before or after L-LTP is induced at a nearby spine. More importantly, there exists a clear branch bias in STC while such a bias has not been demonstrated for crosstalk. These data indicate that crosstalk of E-LTP and the facilitation of L-LTP described here are fundamentally different phenomena. We postulate that the crosstalk phenomenon will also contribute to the Clustered Plasticity phenomenon.

Mechanistically, our data on the distance dependence and branch bias of STC are incompatible with somatic synthesis of PrPs and their subsequent redistribution throughout the dendritic arbor (Barrett et al., 2009; Clopath et al., 2008; Frey, 2001; Frey and Morris, 1997; Okada et al., 2009) unless one assumes the existence of an extra biochemical mechanism that would interact with PrPs, would be restricted to a localized region around the stimulated spine, and would be biased toward operating on the stimulated branch. Instead, the most parsimonious explanation of the observed spatial restriction of STC and the competition between spines for L-LTP expression is that the rate-limiting PrP(s) is synthesized locally (Martin and Kosik, 2002; Steward and Schuman, 2001) and diffuses or is transported to create a gradient away from the PrP synthesis site (Govindarajan et al., 2006). This does not exclude the possibility that rate-nonlimiting PrPs synthesized in the soma contribute to L-LTP formation.

Our findings on L-LTP induction under 1 mM Mg^{+2} conditions imply that there is a threshold of synapse activation below which L-LTP induction does not occur. This threshold could be one of depolarization such as the threshold for dendritic spike initiation, or a biochemical one such as the level of activation of kinases upstream of protein synthesis. Both of these mechanisms are compatible with the branch bias of L-LTP activation that we observed as it has been demonstrated that electrical summation of synaptic inputs can be supralinear within subdendritic domains (Gasparini et al., 2004; Poirazi et al., 2003a, 2003b) and that activation of at least some biochemical pathways can spread over a short distance (Harvey et al., 2008; Yasuda et al., 2006). The mechanism behind why some spines are potentiated after stimulation whereas others are not remains unknown.

We also found that L-LTP induced at one spine facilitates tag formation and consequent L-LTP expression at a neighboring spine where only subthreshold stimulation was given subsequent to the original L-LTP stimulation. This may be caused by one or more of the PrPs altering the excitability locally near the stimulated spines (Johnston and Narayanan, 2008; Williams et al., 2007). The recent demonstration of branch-specific excitability (Losonczy et al., 2008), though not demonstrated to be protein synthesis dependent, supports this hypothesis.

A key consequence of STC is thought to be for binding together, at the single-cell level, of a relatively less prominent or even an incidental event that occurred during a given episode with an important event; less prominent information, encoded initially as E-LTP-like plasticity, will be bound with some important information that would trigger protein synthesis and encoded as L-LTP-like plasticity into one long-term memory episode (Frey, 2001; Govindarajan et al., 2006) via "conversion" of E-LTP to L-LTP. Indeed, recent studies have reported behavioral data that are consistent with the STC hypothesis (Ballarini et al., 2009; Moncada and Viola, 2007). Our finding about the temporal asymmetry of STC suggests that the storage of a piece of less salient information as part of an engram could be affected depending on whether it came before or after the important information. There is a wider time window for less prominent information that arrives before, rather than after, the salient information to be bound together as part of the engram (Figures 3B and 3C). On the other hand, the information can be even less prominent if it comes after the salient event, rather than before, for it to become bound (Figures 3E–3G).

Lastly, our data showing individual branches as the functional unit of long-term memory storage can be used to refine current computational models of STC (Barrett et al., 2009; Clopath et al., 2008), which have incorporated neither the spatial nor competition component of the CPH.

EXPERIMENTAL PROCEDURES

Detailed procedures are given as part of the Supplemental Experimental Procedures. Briefly, mouse organotypic slice cultures were prepared from P7 to P10 animals (Stoppini et al., 1991), and Dendra (Gurskaya et al., 2006) was sparsely introduced via biolistic gene transfection. For acute slice experiments, 300 μm slices were cut from 6- to 9-week-old Thy1-GFP (line GFP-M) (Feng et al., 2000) and used after 3 hr of incubation in an interface chamber. Slices were used between DIV 8 and 16, and were perfused with room temperature ACSF (32°C for acute slices) consisting of 127 mM NaCl, 25 mM NaHCO$_3$, 25 mM D-glucose, 2.5 mM KCl, 1 mM MgCl$_2$, 2 mM CaCl$_2$, 1.25 mM NaH$_2$PO$_4$, and 0.0005 mM TTX (no TTX in Figure S2). Two-photon imaging and glutamate uncaging were performed using a modified Olympus FV 1000 multiphoton microscope with SIM scanner with two Spectra-Physics Mai Tai HP Ti:sapphire lasers. For all electrophysiology experiments, experiments in Figures 4, 6, and 7, spines were chosen only from the most proximal tertiary apical branches (counting the apical trunk as the primary branch). To induce plasticity, an uncaging tetanus was given by positioning the laser 0.5 μm from the tip of the spine head and uncaging MNI-glutamate (2.5 mM) with a stimulus train consisting of either 4 ms (L-LTP, E-LTP) or 1 ms (subthreshold) pulses at 0.5 Hz for 1 min (30 pulses), in the presence (L-LTP) or absence (E-LTP, subthreshold) of 50 μM forskolin or 100 μM SKF38393, the absence of TTX and MgCl$_2$, and the presence of 4 mM (2 mM in Figure S2) CaCl$_2$, and 50 μM picrotoxin (except in Figure S2). For multispine stimulation, fluorescently labeled cells were scanned until one was found in which the first apical tertiary dendrite had multiple spines in the same z plane (generally > 10). Spines were selected, and the experiment was performed only if the stimulations could be done within 6 ms. Stimulations were done as above but with 0.1 ms pulses, 10 mM MNI-Glutamate, 1 mM MgCl$_2$, and 2 mM CaCl$_2$. Each spine received 100 pulses at 2 Hz. The spine stimulation orders were identical throughout the tetani and proceeded from one end to the other. In half the cases, the first stimulated spine was the one closest to the soma, whereas

in other cases it was the one farthest. Protein synthesis, where inhibited, was carried out by the addition of anisomycin (50 μM) or cycloheximide (40 μM) to the ACSF. Uncaging-evoked EPSCs (uEPSCs) were measured using amphotericin B-mediated perforated patch-clamp recordings (Figure 1B) or whole-cell patch clamp (Table 1) and evoked with test stimuli of 1 ms pulses every 10 min at −60 mV. Each time point represents the average value of five trials at 0.1 Hz. Spine volumes were determined by measuring the full width at half maximum (FWHM), representing the diameter of the spine head (Matsuzaki et al., 2004; Tanaka et al., 2008).

SUPPLEMENTAL INFORMATION

Supplemental Information includes Supplemental Experimental Procedures and five figures and can be found with this article online at doi:10.1016/j.neuron.2010.12.008.

REFERENCES

Abel, T., Nguyen, P.V., Barad, M., Deuel, T.A., Kandel, E.R., and Bourtchouladze, R. (1997). Genetic demonstration of a role for PKA in the late phase of LTP and in hippocampus-based long-term memory. Cell 88, 615–626.

Asrican, B., Lisman, J., and Otmakhov, N. (2007). Synaptic strength of individual spines correlates with bound Ca2+-calmodulin-dependent kinase II. J. Neurosci. 27, 14007–14011.

Ballarini, F., Moncada, D., Martinez, M.C., Alen, N., and Viola, H. (2009). Behavioral tagging is a general mechanism of long-term memory formation. Proc. Natl. Acad. Sci. USA 106, 14599–14604.

Barrett, A.B., Billings, G.O., Morris, R.G., and van Rossum, M.C. (2009). State based model of long-term potentiation and synaptic tagging and capture. PLoS Comput. Biol. 5, e1000259.

Chutkow, J.G. (1974). Metabolism of magnesium in central nervous system. Relationship between concentrations of magnesium in cerebrospinal fluid and brain in magnesium deficiency. Neurology 24, 780–787.

Clopath, C., Ziegler, L., Vasilaki, E., Busing, L., and Gerstner, W. (2008). Tag-trigger-consolidation: A model of early and late long-term-potentiation and depression. PLoS Comput. Biol. 4, e1000248.

Feng, G., Mellor, R.H., Bernstein, M., Keller-Peck, C., Nguyen, Q.T., Wallace, M., Nerbonne, J.M., Lichtman, J.W., and Sanes, J.R. (2000). Imaging neuronal subsets in transgenic mice expressing multiple spectral variants of GFP. Neuron 28, 41–51.

Fonseca, R., Nagerl, U.V., Morris, R.G., and Bonhoeffer, T. (2004). Competing for memory; hippocampal LTP under regimes of reduced protein synthesis. Neuron 44, 1011–1020.

Frey, J.U. (2001). Long-lasting hippocampal plasticity: Cellular model for memory consolidation? Results Probl. Cell Differ. 34, 27–40.

Frey, U., and Morris, R.G. (1997). Synaptic tagging and long-term potentiation. Nature 385, 533–536.

Frey, U., and Morris, R.G. (1998). Weak before strong: Dissociating synaptic tagging and plasticity-factor accounts of late-LTP. Neuropharmacology 37, 545–552.

Frey, U., Krug, M., Reymann, K.G., and Matthies, H. (1988). Anisomycin, an inhibitor of protein synthesis, blocks late phases of LTP phenomena in the hippocampal CA1 region in vitro. Brain Res. 452, 57–65.

Frey, U., Schroeder, H., and Matthies, H. (1990). Dopaminergic antagonists prevent long-term maintenance of posttetanic LTP in the CA1 region of rat hippocampal slices. Brain Res. 522, 69–75.

Frey, U., Matthies, H., Reymann, K.G., and Matthies, H. (1991). The effect of dopaminergic D1 receptor blockade during tetanization on the expression of long-term potentiation in the rat CA1 region in vitro. Neurosci. Lett. 129, 111–114.

Frey, U., Huang, Y.Y., and Kandel, E.R. (1993). Effects of cAMP simulate a late stage of LTP in hippocampal CA1 neurons. Science 260, 1661–1664.

Gasparini, S., and Magee, J.C. (2006). State-dependent dendritic computation in hippocampal CA1 pyramidal neurons. J. Neurosci. 26, 2088–2100.

Gasparini, S., Migliore, M., and Magee, J.C. (2004). On the initiation and propagation of dendritic spikes in CA1 pyramidal neurons. J. Neurosci. 24, 11046–11056.

Gelinas, J.N., and Nguyen, P.V. (2005). {beta}-adrenergic receptor activation facilitates induction of a protein synthesis-dependent late phase of long-term potentiation. J. Neurosci. 25, 3294–3303.

Giorgi, C., Yeo, G.W., Stone, M.E., Katz, D.B., Burge, C., Turrigiano, G., and Moore, M.J. (2007). The EJC factor eIF4AIII modulates synaptic strength and neuronal protein expression. Cell 130, 179–191.

Govindarajan, A., Kelleher, R.J., and Tonegawa, S. (2006). A clustered plasticity model of long-term memory engrams. Nat. Rev. Neurosci. 7, 575–583.

Gurskaya, N.G., Verkhusha, V.V., Shcheglov, A.S., Staroverov, D.B., Chepurnykh, T.V., Fradkov, A.F., Lukyanov, S., and Lukyanov, K.A. (2006). Engineering of a monomeric green-to-red photoactivatable fluorescent protein induced by blue light. Nat. Biotechnol. 24, 461–465.

Harvey, C.D., and Svoboda, K. (2007). Locally dynamic synaptic learning rules in pyramidal neuron dendrites. Nature 450, 1195–1200.

Harvey, C.D., Yasuda, R., Zhong, H., and Svoboda, K. (2008). The spread of Ras activity triggered by activation of a single dendritic spine. Science 321, 136–140.

Honkura, N., Matsuzaki, M., Noguchi, J., Ellis-Davies, G.C., and Kasai, H. (2008). The subspine organization of actin fibers regulates the structure and plasticity of dendritic spines. Neuron 57, 719–729.

Huang, Y.Y., and Kandel, E.R. (1994). Recruitment of long-lasting and protein kinase A-dependent long-term potentiation in the CA1 region of hippocampus requires repeated tetanization. Learn. Mem. 1, 74–82.

Johnston, D., and Narayanan, R. (2008). Active dendrites: Colorful wings of the mysterious butterflies. Trends Neurosci. 31, 309–316.

Kang, H., and Schuman, E.M. (1995). Long-lasting neurotrophin-induced enhancement of synaptic transmission in the adult hippocampus. Science 267, 1658–1662.

Kang, H., and Schuman, E.M. (1996). A requirement for local protein synthesis in neurotrophin-induced hippocampal synaptic plasticity. Science 273, 1402–1406.

Kelleher, R.J., 3rd, Govindarajan, A., and Tonegawa, S. (2004). Translational regulatory mechanisms in persistent forms of synaptic plasticity. Neuron 44, 59–73.

Lee, S.J., Escobedo-Lozoya, Y., Szatmari, E.M., and Yasuda, R. (2009). Activation of CaMKII in single dendritic spines during long-term potentiation. Nature 458, 299–304.

Losonczy, A., and Magee, J.C. (2006). Integrative properties of radial oblique dendrites in hippocampal CA1 pyramidal neurons. Neuron 50, 291–307.

Losonczy, A., Makara, J.K., and Magee, J.C. (2008). Compartmentalized dendritic plasticity and input feature storage in neurons. Nature 452, 436–441.

Malenka, R.C., and Bear, M.F. (2004). LTP and LTD: An embarrassment of riches. Neuron 44, 5–21.

Martin, K.C., and Kosik, K.S. (2002). Synaptic tagging—who's it? Nat. Rev. Neurosci. 3, 813–820.

Matsuzaki, M., Honkura, N., Ellis-Davies, G.C., and Kasai, H. (2004). Structural basis of long-term potentiation in single dendritic spines. Nature 429, 761–766.

Moncada, D., and Viola, H. (2007). Induction of long-term memory by exposure to novelty requires protein synthesis: Evidence for a behavioral tagging. J. Neurosci. 27, 7476–7481.

O'Carroll, C.M., and Morris, R.G.M. (2004). Heterosynaptic co-activation of glutamatergic and dopaminergic afferents is required to induce persistent long-term potentiation. Neuropharmacology 47, 324–332.

Okada, D., Ozawa, F., and Inokuchi, K. (2009). Input-specific spine entry of soma-derived Vesl-1S protein conforms to synaptic tagging. Science 324, 904–909.

Otmakhova, N.A., and Lisman, J.E. (1996). D1/D5 dopamine receptor activation increases the magnitude of early long-term potentiation at CA1 hippocampal synapses. J. Neurosci. 16, 7478–7486.

Poirazi, P., and Mel, B.W. (2001). Impact of active dendrites and structural plasticity on the memory capacity of neural tissue. Neuron 29, 779–796.

Poirazi, P., Brannon, T., and Mel, B.W. (2003a). Arithmetic of subthreshold synaptic summation in a model CA1 pyramidal cell. Neuron 37, 977–987.

Poirazi, P., Brannon, T., and Mel, B.W. (2003b). Pyramidal neuron as two-layer neural network. Neuron 37, 989–999.

Sajikumar, S., and Frey, J.U. (2004). Late-associativity, synaptic tagging, and the role of dopamine during LTP and LTD. Neurobiol. Learn. Mem. 82, 12–25.

Sajikumar, S., Navakkode, S., and Frey, J.U. (2008). Distinct single but not necessarily repeated tetanization is required to induce hippocampal late-LTP in the rat CA1. Learn. Mem. 15, 46–49.

Schuman, E.M., Dynes, J.L., and Steward, O. (2006). Synaptic regulation of translation of dendritic mRNAs. J. Neurosci. 26, 7143–7146.

Smith, M.A., Ellis-Davies, G.C., and Magee, J.C. (2003). Mechanism of the distance-dependent scaling of Schaffer collateral synapses in rat CA1 pyramidal neurons. J. Physiol. 548, 245–258.

Smith, W.B., Starck, S.R., Roberts, R.W., and Schuman, E.M. (2005). Dopaminergic stimulation of local protein synthesis enhances surface expression of GluR1 and synaptic transmission in hippocampal neurons. Neuron 45, 765–779.

Steward, O., and Schuman, E.M. (2001). Protein synthesis at synaptic sites on dendrites. Annu. Rev. Neurosci. 24, 299–325.

Stoppini, L., Buchs, P.A., and Muller, D. (1991). A simple method for organotypic cultures of nervous tissue. J. Neurosci. Methods 37, 173–182.

Swanson-Park, J.L., Coussens, C.M., Mason-Parker, S.E., Raymond, C.R., Hargreaves, E.L., Dragunow, M., Cohen, A.S., and Abraham, W.C. (1999). A double dissociation within the hippocampus of dopamine D1/D5 receptor and beta-adrenergic receptor contributions to the persistence of long-term potentiation. Neuroscience 92, 485–497.

Tanaka, J., Horiike, Y., Matsuzaki, M., Miyazaki, T., Ellis-Davies, G.C., and Kasai, H. (2008). Protein synthesis and neurotrophin-dependent structural plasticity of single dendritic spines. Science 319, 1683–1687.

Williams, S.R., Wozny, C., and Mitchell, S.J. (2007). The back and forth of dendritic plasticity. Neuron 56, 947–953.

Yasuda, R., Harvey, C.D., Zhong, H., Sobczyk, A., van Aelst, L., and Svoboda, K. (2006). Supersensitive Ras activation in dendrites and spines revealed by two-photon fluorescence lifetime imaging. Nat. Neurosci. 9, 283–291.